

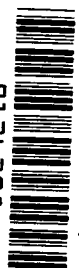
# NASA TECHNICAL NOTE



NASA TN D-8482 *c-1*

NASA TN D-8482

LOAN COPY: RE  
AFWL TECHNICAL  
KIRTLAND AFB

TECH LIBRARY KAFB, NM  
0  
RY  
0134208  


## X-RAY PHOTOELECTRON SPECTROSCOPY STUDY OF RADIOFREQUENCY SPUTTERED CHROMIUM BROMIDE, MOLYBDENUM DISILICIDE, AND MOLYBDENUM DISULFIDE COATINGS AND THEIR FRICTION PROPERTIES

*Donald R. Wheeler and William A. Brainard*

*Lewis Research Center*

*Cleveland, Ohio 44135*

NATIONAL AERONAUTICS AND SPACE ADMINISTRATION • WASHINGTON, D. C. • **AUGUST 1977**





0134208

1. Report No. NASA TN D-8482	2. Government Accession No.	3. Recipient's Catalog No.	
4. Title and Subtitle X-RAY PHOTOELECTRON SPECTROSCOPY STUDY OF RADIOFREQUENCY SPUTTERED CHROMIUM BROMIDE, MOLYBDENUM DISILICIDE, AND MOLYBDENUM DISULFIDE COATINGS AND THEIR FRICTION PROPERTIES		5. Report Date August 1977	6. Performing Organization Code
7. Author(s) Donald R. Wheeler and William A. Brainard		8. Performing Organization Report No. E-9059	
9. Performing Organization Name and Address National Aeronautics and Space Administration Lewis Research Center Cleveland, Ohio 44135		10. Work Unit No. 506-16	11. Contract or Grant No.
12. Sponsoring Agency Name and Address National Aeronautics and Space Administration Washington, D.C. 20546		13. Type of Report and Period Covered Technical Note	
15. Supplementary Notes		14. Sponsoring Agency Code	
16. Abstract <p>Radiofrequency (rf) sputtered coatings of <math>\text{CrB}_2</math>, <math>\text{MoSi}_2</math>, and <math>\text{MoS}_2</math> were examined by X-ray photoelectron spectroscopy (XPS). The effects of sputtering target history, deposition time, rf power level, and substrate bias on film composition were studied. Friction tests were run on rf sputtered surfaces of 440-C steel to correlate XPS data with lubricating properties. Significant deviations from stoichiometry and high oxide levels for all three compounds are related to target outgassing. The effect of biasing on these two factors depended on the compound. Improved stoichiometry correlated well with good friction and wear properties.</p>			
17. Key Words (Suggested by Author(s)) Sputtering ESCA Refractory Coatings		18. Distribution Statement Unclassified - unlimited STAR Category 24	
19. Security Classif. (of this report) Unclassified	20. Security Classif. (of this page) Unclassified	21. No. of Pages 21	22. Price* A02

X-RAY PHOTOELECTRON SPECTROSCOPY STUDY OF RADIOFREQUENCY  
SPUTTERED CHROMIUM BROMIDE, MOLYBDENUM DISILICIDE, AND  
MOLYBDENUM DISULFIDE COATINGS AND THEIR FRICTION PROPERTIES

by Donald R. Wheeler and William A. Brainard

Lewis Research Center

SUMMARY

X-ray photoelectron spectroscopy (XPS) was used to analyze rf sputtered film, of  $\text{CrB}_2$ ,  $\text{MoSi}_2$ , and  $\text{MoS}_2$ . XPS data provided information on stoichiometry, impurity content, and chemical bonding. The influences of sputtering target history, deposition time, rf power level, and substrate bias on the film composition were studied. Friction tests were run on 440-C steel sputter-coated with the same films to relate XPS data to lubricating properties.

Significant variations in both stoichiometry and impurity content were observed for all three materials. Films sputtered from  $\text{CrB}_2$  targets varied from mixtures of chromium and boron oxides to nearly stoichiometric chromium boride films depending on target history. This is related to the presence of an oxidized surface layer which must be removed before the bulk target material can be sputtered. Increased rf power and deposition time also produced poor quality films due to target heating. The heating caused gaseous diffusion from the bulk of the porous hot-pressed target to the surface. Substrate biasing improved both stoichiometry and purity for  $\text{CrB}_2$ .

$\text{MoSi}_2$  was little effected with regard to stoichiometry by biasing but both oxygen and carbon contents were reduced.

$\text{MoS}_2$  showed severe sulfur depletion when bias deposited. Sulfur content on a sample deposited with 500-volt bias, was less than 10 percent of the standard value. Films with low sulfur content had high oxygen concentration because the excess molybdenum left in the compound getters oxygen. The oxidation of molybdenum is confirmed by shifts in the XPS spectra.

Films which were most nearly stoichiometric exhibited good friction and wear characteristics. High oxide levels did not appear to influence the friction results unless the film stoichiometry was also poor.

## INTRODUCTION

Sputtering is being used in an increasing number of applications. Both thin and thick films are being deposited as the versatility of the method becomes more recognized by industry. In particular, sputtering has found extensive application in such areas as electronics, corrosion protection, decorative coatings, catalysis, antiwear coatings, and solid film lubrication (ref. 1).

In the field of tribology thin films of pure metal, metallic alloys, inorganic compounds, and plastics are sputtered routinely. Refractory carbides and silicides are sputtered onto bearing steels to improve wear life and softer compounds like molybdenum disulfide and PTFE are used as low shear strength lubricant films (ref. 2).

Many observers have noted that significant differences in coating properties occurred depending on the deposition conditions. For example, the electrical resistivity of metallic films varied widely depending on degree of substrate bias. The structure and growth characteristics of compounds was found to depend on pressure and power level (refs. 3 and 4). In the field of lubrication, molybdenum disilicide films showed poor adherence and thus poor antiwear properties until a substrate bias was applied during film deposition (ref. 5). Spalvins in his work on the sputtering of molybdenum disulfide, showed that a chemical reaction between the depositing  $\text{MoS}_2$  film and copper and silver substrates occurred resulting in poor adherence and lubricating properties; whereas when other metal substrates were used, good adherence and lubricating ability was achieved (ref. 6).

In view of the importance of these observations to tribology and also due to the importance of the chemistry or purity of sputtered films in other areas such as electronics or catalysis, a study of the chemistry of sputtered films was undertaken.

Chemical analyses of sputtered films are infrequently done. Rather, indirect measurements such as resistivity are more often employed. Direct measurements either require prohibitively thick films or removal of the film from the substrate - often difficult and tedious (ref. 7). X-ray photoelectron spectroscopy (XPS) is ideally suited to the study of sputtered film composition. Because it is surface sensitive, thin films can be studied without elaborate preparation. When used in conjunction with sputter etching, XPS can provide information on variations of composition with depth. Information on chemical bonding as well as composition is available by observing shifts of the electron binding energies (ref. 8).

The objective of this investigation was to use XPS to characterize radiofrequency (rf) sputter deposited films of materials that are of current interest in the field of lubrication. The materials studied were molybdenum silicide ( $\text{MoSi}_2$ ), chromium boride ( $\text{CrB}_2$ ), and molybdenum sulfide ( $\text{MoS}_2$ ) deposited on 440-C steel. The variations of stoichiometry and impurity content were studied as functions of target history, bias

voltage, power level, and sputtering time.

Friction and wear tests using a pin on disk apparatus were done in an attempt to correlate XPS data with frictional properties. RF sputter deposited films were tested on 440-C stainless steel substrates in a nitrogen atmosphere.

## APPARATUS AND PROCEDURE

### Radiofrequency Sputtering Apparatus

The sputtering of the materials used in this investigation was conducted in a commercial rf diode apparatus operating at 13.56 MHz. The apparatus is shown schematically in figure 1. The material to be sputter deposited is in the form of a hot-pressed disk-shaped compact, 15.2 centimeters in diameter which was commercial purchased. The compact or target as it is called when mounted, is cemented with a silver conductive epoxy onto a copper backing plate (10.60 cm thick). The copper backing plate is mounted onto a water cooled rf electrode also 15.2 centimeters in diameter. The specimen to be coated is placed 2.5 centimeters directly below the target on an electrically insulated block. The insulated block sets on the grounded substrate table. (The target and the grounded table comprise the rf diode.) An additional voltage from 0 to -1500 volts dc may be applied directly to the specimen either for specimen cleaning by dc sputter etching or for biasing the specimen during film deposition and growth.

Provision is made for rotation of the entire substrate table so the specimen may be moved out from under the target for cleaning. The target also can be cleaned in this manner without contaminating the specimen.

The entire system comprising the diode is contained in a glass bell jar, 45 centimeters in diameter. The system is mechanically fore-pumped and oil diffusion pumped through a liquid nitrogen cooled baffle. During deposition, high purity argon (99.999 percent) was bled continuously into the system through a leak valve and a dynamic pressure balance between the pumping system and argon leak of approximately 20 microns was maintained in the bell jar.

Prior to actually starting deposition, the target and specimen were cleaned. The target was cleaned first by rf sputtering it until little pressure rise due to outgassing occurred. This was coincident with the plasma taking on a blue-green coloration for the  $\text{MoSi}_2$  and  $\text{CrB}_2$  targets. No pronounced coloration was observed with the  $\text{MoS}_2$  target. Following target cleaning, the rf was turned off and the 440-C disk specimen cleaned by dc sputter etching at -1200 volts for 15 minutes. Following specimen cleaning, the selected power and bias voltage parameters were set and the specimen rotated back under the target and deposition initiated.

## X-ray Photoelectron Spectroscopy

General principles. - After deposition, the films were analyzed by X-ray photoelectron spectroscopy (XPS). The principles of XPS are detailed in references 8 and 9. Briefly, X-ray photons striking an atom in the surface cause it to emit an electron. The electron will leave the atom with a kinetic energy  $K$ , which is the difference between the incident photon energy  $h\nu$  and the binding energy  $E_B$  of the electron in the atom. The binding energy is characteristic of the atom excited and depends on the oxidation state of the atom. Thus, if the electron energies  $K$  emitted from a sample are measured and  $h\nu$  is known, the atoms in the sample may be identified and information about the compounds in which they exist extracted by comparing the measured binding energies with binding energies measured previously on standard samples. Because of the low kinetic energies (less than 2 keV) of the electrons, the atoms more than 20 Å below the surface of a solid do not contribute to the spectrum.

The intensity of electron emission from any energy level in a particular chemical species is proportional to the photoelectric cross section for that level, the escape depth of the electrons in the sample and the concentration of that species. The cross section is different for every energy level in every atom, but does not vary with the oxidation state of the atom. The escape depth depends on the electron's kinetic energy and the absorption properties of the specimen as a whole: the so-called matrix effects. The technique is thus semiquantitative.

Apparatus. - The particular apparatus used here consisted of a commercial electron energy analyzer, described in reference 10, and an X-ray source in a vacuum system designed to accommodate a variety of samples. The system is a stainless steel bakeable ultrahigh vacuum system. It is ion pumped and incorporates a titanium sublimation pump. An ion gun in the system was used to gradually sputter away the sample surface and determine the composition as a function of depth. The configuration of the system is shown schematically in figure 2(a).

The X-ray source had a magnesium target with a characteristic energy,  $h\nu$ , of 1253.6 eV. It was operated at 10 kV and 40 mA and is regulated in such a way that the X-ray flux is held constant despite voltage fluctuations. The electron energy analyzer is a retarding grid followed by a double pass cylindrical mirror analyzer (CMA) whose axis is normal to the X-ray beam. The energy of electrons passed by the CMA is fixed (50 eV here), and the retarding grid voltage is increased linearly with time. This voltage drives the x-axis of an x-y recorder. Electrons passing through the CMA cause pulses in an electron multiplier. These pulses are fed to a ratemeter which drives the y-axis of the x-y recorder. The recorder thus plots a spectrum which consists of electrons per second against energy. A block diagram of the apparatus is given in figure 2(b).

Each energy level in every atom in the analyzed region contributes an electron peak at its binding energy. These peaks are identified by the usual spectroscopic notation in the discussion and figures to follow. Thus the position of each peak in the spectrum identifies an element present in the sample surface and gives some information about the oxidation state of that element. The height of the peak is related to the amount of the element presented in the surface.

Data analysis and calibration. - The peak widths depend on the pass energy of the CMA. In this study, peak widths are no less than 1.5 eV full width at half maximum. The peak maxima can be located to  $\pm 0.1$  eV at best. The energies are referenced to the carbon (1s) line at 284.0 eV and location of this line adds  $\pm 0.2$  eV to the energy uncertainty. Therefore  $\pm 0.3$  eV is a reasonable estimate of the probable error of the binding energies quoted here. The reproducibility of peak height values was determined by measuring several characteristic peaks from a sputter deposited film at six different locations on the film. The probable error in the peak heights ranged from  $\pm 2$  to  $\pm 10$  percent, the larger value being for peaks near the limits of detectability. Peak ratios were generally good to  $\pm 10$  percent or less.

Because the chemical shifts in binding energy are sometimes comparable to the width of the peak, a peak is frequently broadened without being resolved into two distinct peaks. In most cases these broadened peaks could be resolved using an analog curve resolver. In this way binding energies and peak heights for all components of a peak could be obtained.

The binding energy characteristics of an element in a particular compound must be determined by measurement on that compound. Table I lists the binding energies determined for compounds that will be of interest here. The oxygen peak height was always between 529 and 531 eV. Since the samples were always sputter-cleaned before analysis, this is taken to be an oxide peak. Reference will also be made to the ratios of peak heights in  $\text{CrB}_2$ ,  $\text{MoSi}_2$ , and  $\text{MoS}_2$ . These peak heights were determined by XPS measurement on standards of those materials.

Procedure. - The procedure used for XPS analysis was the same for all samples. The surface was rinsed with alcohol before the specimen was installed in the vacuum system. The pressure was allowed to reach  $10^{-5}$  N/m<sup>2</sup> before any analysis was undertaken. Each type of material was sputter etched before analysis with argon ions for a time which previous trials had shown was sufficient to remove the surface contaminant layers and expose the bulk coating material.

The ion gun is a commercial unit operated at an ion energy of 2 keV. During sputter etching, the vacuum system is backfilled to  $7 \times 10^{-3}$  N/m<sup>2</sup> with argon gas. The titanium sublimation pump in the system is operated periodically to maintain the gas purity.

## Friction Apparatus

The testing of the rf sputtered films was done on a pin or disk apparatus. The pin or disk configuration is widely used for solid film lubrication testing and details of this particular apparatus are available in the literature (ref. 5).

Briefly stated, the apparatus consists of a flat 6.4-centimeter-diameter disk which is mounted on the end of a rotative shaft. The disk specimen is a type 440-C stainless steel disk which has been rf sputtered coated with one of the test materials and is used as it comes from the XPS system after analysis.

Loaded against the surface of the disk is a 0.476-centimeter-radius pin of 304 stainless steel. The pin is mounted in a holder on the end of and perpendicular to a gimbal supported arm. The pin is loaded against the surface of the disk by hanging weights on the arm halfway between the pin and gimbal. The end of the arm opposite the pin holder is attached to a strain gage bridge, which measures the frictional force.

The entire apparatus is enclosed in a clear plastic box. A constant flow of dry nitrogen is maintained in the box prior to and during frictional tests to minimize environmental effects.

The tests reported in this report were conducted at a constant speed of 25 centimeters per second. The loads used were 10 to 25 grams force ( $(9.8 \text{ to } 24.5) \times 10^{-2}$  N). Tests were run until an equilibrium friction value was achieved or until the film failed.

## RESULTS

### Chromium Boride

Target history. - A  $\text{CrB}_2$  target was exposed to air for 2 days. Then a series of films were prepared. Successive films were deposited after increasing target sputter cleaning times. The vacuum system was not opened between depositions. No bias voltage was used.

Figure 3 shows the boron XPS spectra of these films. The film deposited after only 30 minutes of target sputtering contains virtually no boride but only boron oxide. The amount of boride increases with increasing target sputtering. The chromium spectrum showed a similar change from a chromium oxide to a boride as the series progressed. It was observed that the color of the glow discharge in the sputtering system changed as the series progressed. It was first a purple color and changed gradually to a brighter blue. Furthermore it was noticed that the base pressure in the vacuum system when the argon flow was stopped was an appreciable part of the sputtering pressure early in the series becoming negligible at the end.



The  $\text{CrB}_2$  target is a particularly porous pressed compact. It is concluded that the results here are due to degassing of this porous target. This effect has been observed with hot pressed targets by Vossen (ref. 11). In all the work reported hereinafter, the importance of degassing the target was recognized. It was found that by monitoring the color of the glow discharge and only depositing coatings after the color had stabilized, reproducible coatings be applied. No other target showed as great a propensity to outgas as did the  $\text{CrB}_2$ .

Substrate bias. - Coatings were prepared with the substrate held at bias voltages from 0 to -500 volts. In general the XPS spectra from these coatings showed a pair of clearly resolved boron (1s) peaks at 187.6 and 191.5 eV similar to those of figure 3 and a broad chromium (2p 3/2) peak. The  $\text{Cr}(2p\ 3/2)$  peak was resolved using the analog curve resolver into a  $\text{CrB}_2$  peak at 573.6 eV and a broad  $\text{Cr}_2\text{O}_3$  peak at 576.0 eV. The broadening of the chromium peak in  $\text{Cr}_2\text{O}_3$  is commonly observed (ref. 13). In addition to the chromium and boron spectra, the O(1s) and C(1s) spectral lines were recorded.

In order to show the effect of bias voltage on chromium boride stoichiometry the ratio of the 187.6 eV B(1s) and 573.6 eV  $\text{Cr}(2p\ 3/2)$  peak heights was plotted as a function of bias voltage and compared to the same ratio for the  $\text{CrB}_2$  standard. The result is figure 4(a). Figure 4(b) shows the variation in oxygen peak height with bias voltage. The boron oxide B(1s) peak (191.5 eV) decreases exactly as the oxygen peak does. The carbon peak was unaffected by biasing.

It can be seen from figure 4 that biasing in the range of -100 to -300 volts produces improved stoichiometry of the chromium boride although the composition of the target material is never achieved.

Deposition time. - Figure 4 also shows the effect of reducing the deposition time (and hence the film thickness) from 20 minutes to 10 minutes. There is a distinct reduction in oxygen content and a corresponding improvement in stoichiometry at lower bias voltages. At -300 and -500 volts there is no difference.

Figure 5 shows a clear correlation between compound stoichiometry and the oxygen content of the film. However, it is also clear from figures 4 and 5 that something other than oxygen influences stoichiometry at -500 volts bias. The chromium boride never reaches the target stoichiometry and at high bias voltage it deteriorates in spite of decreasing oxygen content.

Sputtering power. - A  $\text{CrB}_2$  film was deposited with -500 volts bias for 10 minutes at 600 watts target power instead of the 300 watts used for the other films. Figure 6 shows how the oxygen, boron, and boride peak heights varied with depth in this film. Figure 7 shows the change in the  $\text{Cr}(2p\ 3/2)$  peak with depth. The peak has been resolved into its oxide and boride components. The coating is entirely chromium oxide and boron oxide in its outer surface. After 80 minutes of ion beam etching the oxide

decreases and some boride appears. After 120 minutes of etching, the film is primarily boride. At this depth the boride to chromium peak height ratio is identical to that of -500 volts bias films deposited at 300 watts.

Summary of CrB<sub>2</sub> results. - While an initial presputtering of targets is common practice in order to clean the surface and reach equilibrium, the degree of outgassing from a porous compact like CrB<sub>2</sub> necessitates extreme care. Deposited films have been found to be oxidized to some degree due to outgassing caused by insufficient presputtering of the target, long sputtering times, and high power levels.

Bias sputtering had two effects on the CrB<sub>2</sub> coatings. Oxides were decreased and the stoichiometry of the chromium boride improved by increasing the bias voltage from 0 to -300 volts. Stoichiometry was adversely affected by bias voltages from -300 to -500 volts.

### Molybdenum Disilicide

Figure 8 shows the effect of bias voltage on the silicon XPS peak. The broad shoulder near 102 eV could be attributed to SiO<sub>2</sub>, SiC, or both. Films deposited without presputtering the target showed only SiO<sub>2</sub>.

Figure 9(a) shows that oxygen and carbon are both present. As the bias voltage is increased there is a rapid initial decrease in the oxygen peak while the carbon peak is little changed. The 102 eV silicon peak also shows a rapid initial decrease. Thus the 102 eV peak is almost certainly due to silicon oxide. The peak is broadened toward lower binding energy. This is probably because the oxide is not stoichiometric SiO<sub>2</sub>. It is not unusual to find a range of composition in silicon oxide films whether thermally grown or sputtered (refs. 14 and 15).

The binding energy of the Mo(3d 5/2) peak was 227.5 eV for all the samples. Since molybdenum in oxide form has a 3d 5/2 binding energy in the 231.0 to 232.5 eV range, there is very little molybdenum oxide present in these films, and the 227.5 eV peak is attributed to molybdenum either free or as the silicide.

Figure 9(b) shows the effect of bias on the ratio of the silicide peak to the molybdenum peak. Comparison with the pressed compact that was used as a standard indicates the degree of stoichiometry in the MoSi<sub>2</sub> component of the film. Clearly bias voltages up to -100 volts make a substantial improvement in the film composition.

### Molybdenum Disulfide

The MoS<sub>2</sub> target was easily degassed by presputtering. The color of the glow discharge stabilized quickly and the base pressure was low even when the target was hot.

The film compositions were very reproducible.

Figure 10(a) shows the effect of substrate bias on film stoichiometry as indicated by the sulfide (162.8 eV) to molybdenum peak height ratio. The 162.8 eV peak was the only detectable sulfur peak. Figure 10(b) shows the oxygen peak height as a function of bias voltage. Table II shows the values of the Mo(3d 5/2) binding energy at the bias voltages used.

At zero bias voltage the deposited film is MoS<sub>2</sub>. There is some oxygen present as an oxide of molybdenum. This would account for the slightly low value of the sulfide to molybdenum ratio. No sulfates were detected.

As the bias voltage is increased, there is resputtering of both oxygen and sulfur. Sulfur decreases with increasing bias voltage until at -500 volts, there is very little sulfur present in the coating. However, by -300 volts the oxygen level has begun to increase again and at -500 volts it is actually greater than it was at 0 volt. The trend of the Mo(3d 5/2) binding energy (table II) toward higher values is consistent with oxidation of the molybdenum. The fact that it does not reach the value of 230.9 eV characteristic of MoO<sub>2</sub> indicates that the Mo is not all oxidized. The remainder probably being present as metallic Mo.

### Friction Results

After the coated samples were analyzed in the XPS system, they were run on the pin on disk apparatus to determine the friction behavior. The chromium boride samples which were prepared as a function of target cleanup time showed a decrease in friction corresponding to an increase in cleanup time as shown in figure 11. The drop in friction is directly related to the changes in the chemistry of the sputtered coating (refer to fig. 3). The first sample, done at 30 minutes target cleanup time, was primarily chromium oxide and boron oxide. With increasing time (76 min) the chemistry changes to a mixture of oxides and chromium boride. This is reflected in a decrease in the friction. Finally at 120 minutes cleanup time, the coating was essentially pure boride. This coating yielded the lowest film friction.

Figure 4 shows that the best stoichiometry of the CrB<sub>2</sub> coatings occurred at -300 volts bias while the worst was at 0 volt bias. Further the deposition time is a factor in composition; those films deposited with longer deposition times are poorer in quality than those done in shorter times (thinner films). Samples done at 0 and -300 volts bias are compared in figure 12. They were extra thick films taking 40 minutes to deposit (~6000 to 7000 Å). The combination of long deposition time coupled with no bias yield a poor film which showed high friction and wear. The film done at -300 volts bias, while also done for 40 minutes, was sufficiently improved by the application of bias to

yield a film with good friction and wear properties.

Figure 13 shows how friction varied with bias voltage for the molybdenum compounds. The  $\text{MoSi}_2$  coatings had the same friction over the entire range. This is consistent with the data of figure 9(b) which showed that very little deviation in stoichiometry occurred for the silicide over the entire range of bias voltages. The decrease in silicon oxide and carbon levels, figure 9(a) do not appear to be significant with regard to the friction as measured by these tests.

Figure 13 shows that the  $\text{MoS}_2$  friction is low ( $<0.10$ ) for 0- and -100-volt bias samples but at -300 and -500 volts, high friction is measured. This obviously is related to the large deviations from stoichiometry that occur at these voltages. The sulfide to molybdenum ratio of the -300-volt sample is only one-third the standard value; while for the -500-volt sample, the ratio is even lower, less than one-tenth the standard.

## DISCUSSION

### Deposition Time, Sputtering Power, Target Preparation

The purity of the sputtered material, especially its oxygen content, is influenced by all three aforementioned factors. It is proposed that oxygen contamination has two sources in the target.

First, there is an oxidized layer at the surface. This source may be more important for pressed compacts than for cast targets because of the high surface to volume ratio of the compacts. The long cleanup times for the  $\text{CrB}_2$  target (fig. 3) and the pure oxide that is deposited initially from both the  $\text{CrB}_2$  and  $\text{MoSi}_2$  targets are evidence for such an oxide layer as the initial source of oxygen contamination.

Once the initial oxide layer has been removed, the second source of oxygen is diffusion from the bulk of the target. Once again this is obviously especially significant for targets made of pressed powders. During the target cleanup, a region near the surface of the target is degassed. Films deposited after this are relatively free of oxide; however, there is always some residual contamination due to further diffusion from the bulk.

If the sputtering power is high, the target temperature will rise causing much more rapid diffusion. The result is a deterioration of the film as sputtering goes on. This was seen in the depth profile (fig. 6) of the  $\text{CrB}_2$  film deposited at 600 watts.

Even at lower power the oxygen continually diffuses to the surface, after the initial cleanup. Furthermore as sputtering progresses, the surface of the target gradually recedes into the more heavily contaminated bulk. Both of these things cause films

with long deposition times to be more heavily oxidized than films with shorter deposition times. This is clearly the case for the 20-minute  $\text{CrB}_2$  films as opposed to the 10-minute films (fig. 4).

To summarize, pressed compact targets yield highly oxidized films because of their oxidized surface and included oxygen. Proper target preparation can remove the surface oxide and degas the surface region of the target allowing deposition of purer films. High power levels and long deposition times, by increasing diffusion rates and exposing more poorly degassed bulk material, cause more contaminated films. In any case, oxygen is always a significant contaminant in films deposited without substrate bias. This is evident in the curves of oxygen versus bias voltage for all three materials tested.

### Substrate Bias Voltage

When the substrate is biased with a negative voltage during deposition, there will be some sputtering of the substrate surface as the film is deposited. This will cause resputtering of atoms from the film. In a multicomponent film, such as those discussed here, the sputtering rates of the two components may differ. In that case the film will become deficient in the component with the higher sputtering yield.

Unfortunately, measured sputtering yields from multicomponent films are not available. However, by using the ion gun in the XPS system to sputter etch  $\text{MoS}_2$  films it was determined that sulfur was sputtered more rapidly from these films than was molybdenum. The sulfur to molybdenum XPS peak height ratio decreased from 0.24 after 30 seconds of sputtering to 0.15 after 20 minutes sputtering. The  $\text{CrB}_2$  and  $\text{MoSi}_2$  films showed no comparable change in composition with sputtering time.

From these observations it is expected that the composition of  $\text{MoS}_2$  would be most strongly affected by bias voltage. That is, in fact, the case as can be seen by comparing figures 4(a), 9(b), and 10(a). The stoichiometry of  $\text{MoSi}_2$  is unaffected by bias voltage. There is some evidence of a small effect on  $\text{CrB}_2$  in the decrease in peak height ratios at high bias voltage. The  $\text{MoS}_2$  films however show an almost total loss of sulfur at -500 volts bias.

A second effect of bias voltage is the decrease in oxygen content of the films as the bias voltage is increased. This is a commonly observed phenomenon (ref. 14) and is of particular value for these pressed compact targets which tend to produce oxidized films. The reason for the preferential sputtering of oxygen is not known. It is known that many metal oxides are reduced by sputtering (refs. 16 and 17) so that the sputtering yield for oxygen is apparently relatively high. In any case, removal of oxygen from the film as it is forming can improve the stoichiometry of the deposited compound

as is the case for  $\text{CrB}_2$  (fig. 5).

The  $\text{MoS}_2$  film is unique in showing an increase in oxygen content at high bias voltages (fig. 10(b)). This may be because of the large decrease in sulfur content of the film. The free molybdenum remaining, which has a great oxygen affinity, could react with oxygen in the sputtering chamber or after exposure to air. The binding energy of the molybdenum shows evidence for oxide formation at high bias voltage.

Thus the effect of biasing on film composition depends strongly on the particular compound being deposited and on the choice of bias voltage. For  $\text{MoSi}_2$ , any bias voltage reduced the oxide content, and the stoichiometry remained good. The stoichiometry of  $\text{CrB}_2$  was actually improved by bias voltages up to -300 volts and degraded at -500 volts while the oxygen content decreased at all bias voltages. The use of bias voltages for  $\text{MoS}_2$  drastically degraded the film stoichiometry and even caused an increase in oxygen content at -500 volts.

### Friction Results

The results of the friction tests reflect the stoichiometry of the films as revealed by XPS. When the film stoichiometry improves, friction is lower as seen in figures 11 and 12 and for  $\text{MoS}_2$  in figure 13. The stoichiometry of  $\text{MoSi}_2$  is the same for all samples as is the friction. Apparently the oxide content as such is not important since the  $\text{MoSi}_2$  friction was not affected by it. As it influences stoichiometry as in  $\text{CrB}_2$ , however, it has a strong effect.

### CONCLUSIONS

Based on the analysis with X-ray photoelectron spectroscopy (XPS) on radiofrequency (rf) sputtered films of  $\text{CrB}_2$ ,  $\text{MoSi}_2$ , and  $\text{MoS}_2$ , the following conclusions are offered:

1. The stoichiometry and impurity content of rf sputtered films greatly depend on target history, deposition time, and power level.
2. Oxygen liberated from the oxidized surface layer and from bulk outgassing of the hot pressed targets is the major impurity.
3. Applying a dc bias voltage during deposition, in general, reduces the oxide content.
4. With regard to film stoichiometry, the effect of bias voltage is specific to each compound.  $\text{MoSi}_2$  was little affected; the stoichiometry of  $\text{CrB}_2$  was significantly im-

proved while for MoS<sub>2</sub> preferential back sputtering of S resulted in sulfur deficient films.

5. Good correlation of XPS data on stoichiometry and friction performance were obtained. Little effect of oxide content was seen for these materials under test conditions.

Lewis Research Center,  
National Aeronautics and Space Administration,  
Cleveland, Ohio, May 11, 1977,  
506-16.

#### REFERENCES

1. Thornton, J. A.: Sputter Coating - Its Principles and Potential. SAE Paper 730544, May 1973.
2. Spalvins, T.: Sputtering. NASA TM X-73527, 1976.
3. Vossen, J. L.: Control of Film Properties by RF-Sputtering Techniques. J. Vac. Sci. Technol., vol. 8, no. 5, 1971, pp. S12-S30.
4. Maissel, L.: Application of Sputtering to the Deposition of Films. Handbook of Thin Film Technology, L. I. Maissel and R. Glang, eds., McGraw-Hill, 1970, pp. 4-1 to 4-44.
5. Brainard, William A.: Friction and Wear Properties of Three Hard Refractory Coatings Applied by Radiofrequency Sputtering. NASA TN D-8484, 1977.
6. Spalvins, Talivaldis: Morphological Growth of Sputtered MoS<sub>2</sub> Films. ASLE Trans., vol. 19, no. 4, 1976, pp. 329-334.
7. Pliskin, W. A.; and Zanin, S.: Film Thickness and Composition. Handbook of Thin Film Technology, L. I. Maissel and R. Glang, eds., McGraw-Hill, 1970, pp. 11-1 to 11-54.
8. Siegbahn, Kai, et al.: ESCA - Electron Spectroscopy for Chemical Analysis. Alinquist and Wiksel (Uppsala), 1967.
9. Swingle, Robert S., II; and Riggs, William M.: ESCA. Crit. Rev. Anal. Chem., vol. 5, no. 3, Oct. 1975, pp. 267-321.
10. Palmberg, P. W.: A Combined ESCA and Auger Spectrometer. J. Vac. Sci. Technol., vol. 12, no. 1, Jan./Feb. 1975, pp. 379-384.

11. Vossen, J. L.: Contamination in Films Sputtered from Hot-Pressed Targets. *J. Vac. Sci. Technol.*, vol. 8, no. 6, 1971, pp. 751-752.
12. Robinson, J. W., ed.: Handbook of Spectroscopy. Vol. I. CRC Press, 1974.
13. Carver, J. C.; Schweitzer, G. K.; and Carlson, Thomas A.: Use of X-ray Photoelectron Spectroscopy to Study Bonding in Cr, Mn, Fe, and Co Compounds. *J. Chem. Phys.*, vol. 57, no. 2, July 15, 1972, pp. 973-982.
14. Christensen, Orla: Characteristics and Applications of Bias Sputtering. *Solid State Technol.*, vol. 13, no. 12, Dec. 1970, pp. 39-45.
15. Johannessen, J. S.; Spicer, W. E.; and Strausser, Y. E.: Phase Separation in Silicon Oxides as Seen by Auger Electron Spectroscopy. *Appl. Phys. Lett.*, vol. 27, no. 8, Oct. 15, 1975, pp. 452-454.
16. Kim, K. S.; and Winograd, Nicholas: X-ray Photoelectron Spectroscopic Studies of Nickel-Oxygen Surfaces Using Oxygen and Argon Ion-Bombardment. *Surf. Sci.*, vol. 43, no. 2, June 1974, pp. 625-643.
17. Kim, K. S.; et al.: X-ray Photoelectron Spectroscopic Studies of lead (II) oxide Surfaces Bombarded with Helium (1+), Neon (1+), Argon (1+), Xenon (1+), and Krypton (1+). *Surf. Sci.*, vol. 55, no. 1, 1976, pp. 285-290.



TABLE I. - BINDING ENERGIES USED AS STANDARDS

Element	Level	Compound	Binding energy, eV	Reference
Si	2p	MoSi <sub>2</sub>	99.1	Measured from MoSi <sub>2</sub> pressed compact
		SiC	102.0	Ref. 12
		SiO <sub>2</sub>	103.0	Ref. 12
S	2p	MoS <sub>2</sub>	162.8	Measured from natural molybdenite
B	1s	CrB <sub>2</sub>	187.6	Measured from target material
		B <sub>2</sub> O <sub>3</sub>	191.5	Measured from B <sub>2</sub> O <sub>3</sub> powder
Mo	3d 5/2	MoSi <sub>2</sub>	227.4	Measured from MoSi <sub>2</sub> pressed compact
		Mo	227.6	Measured from Mo foil
		MoO <sub>2</sub>	230.9	Ref. 12
		MoO <sub>3</sub>	232.5	Ref. 12
Cr	2p 3/2	CrB <sub>2</sub>	573.6	Measured from target material
		CrO <sub>3</sub>	576.0	Ref. 13

TABLE II. - Mo (3d 5/2) BINDING ENERGY IN

MoS<sub>2</sub> AND MOLYBDENUM OXIDES

Specimen	Bias voltage, V	Binding energy, eV
Molybdenite	----	228.3
Sputtered film	0	228.4
Sputtered film	-100	228.8
Sputtered film	-300	229.2
Sputtered film	-500	229.1
MoO <sub>2</sub>	----	230.9
MoO <sub>3</sub>	----	232.5

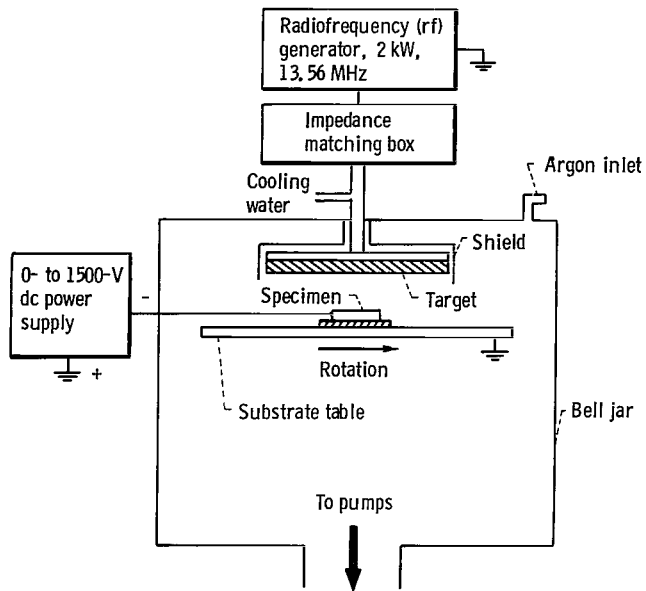
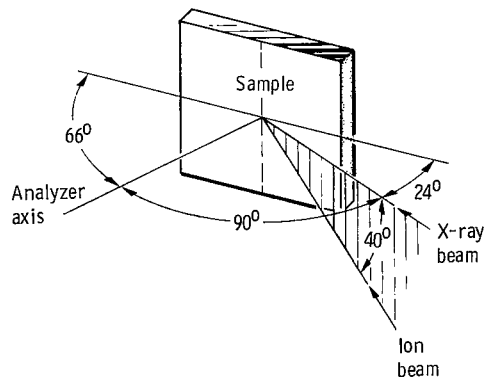
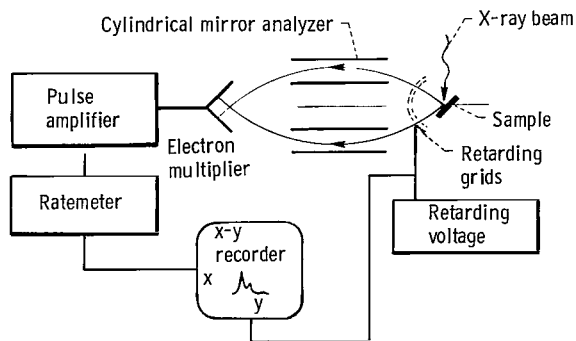


Figure 1. - Schematic of rf sputtering apparatus.



(a) Geometry of system.



(b) Block diagram.

Figure 2. - Configuration of XPS system.

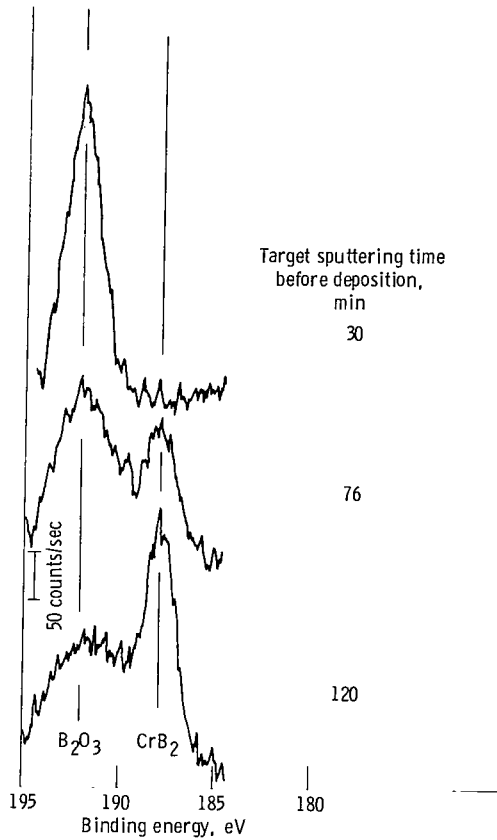


Figure 3. - Change in boron XPS peak with target use.  $\text{CrB}_2$  target substrate grounded. Peaks recorded after 5-minute ion etching. (See table I for  $\text{B}_2\text{O}_3$  and  $\text{CrB}_2$  binding energies.)

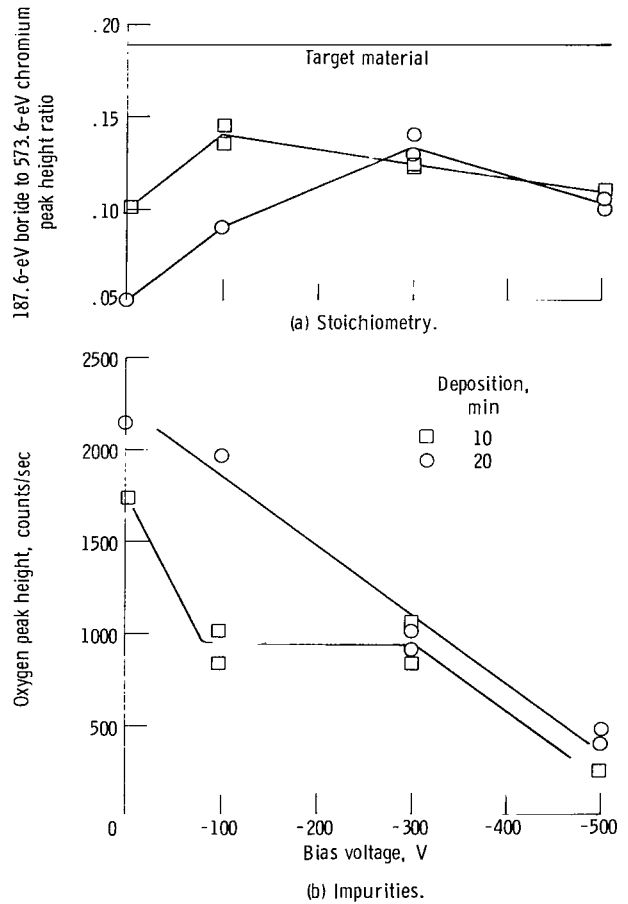


Figure 4. - Influence of bias voltage on  $\text{CrB}_2$  coatings.

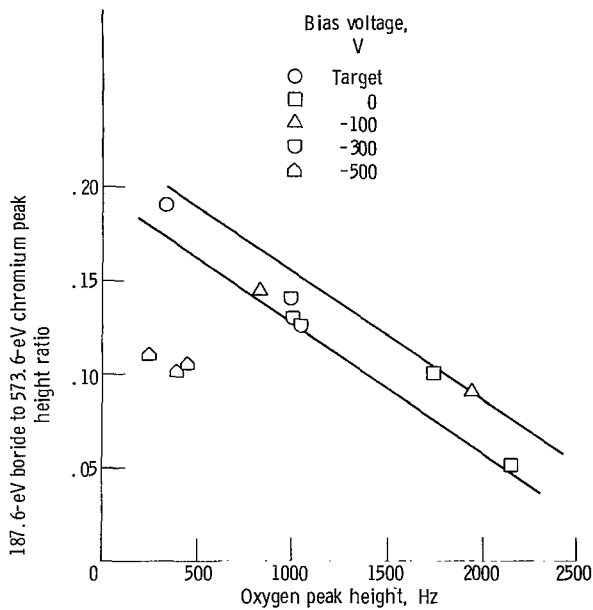


Figure 5. - Boride- to chromium ratio for sputtered  $\text{CrB}_2$  films as a function of oxygen content.

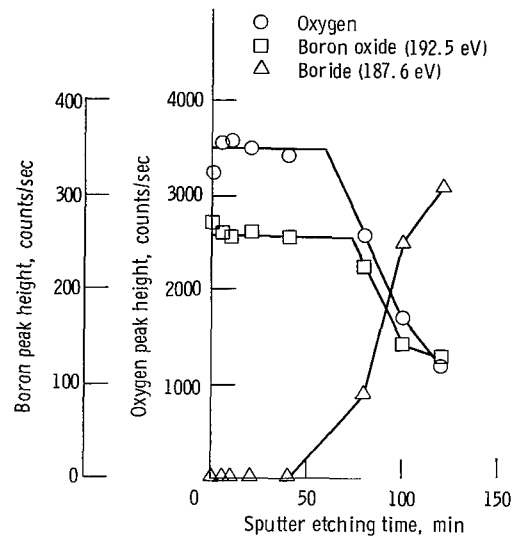


Figure 6. - XPS peak heights as a function of 2-keV argon ion etch time for  $\text{CrB}_2$  coating; 600 watts; 10 minutes deposition time; -500 volts bias.

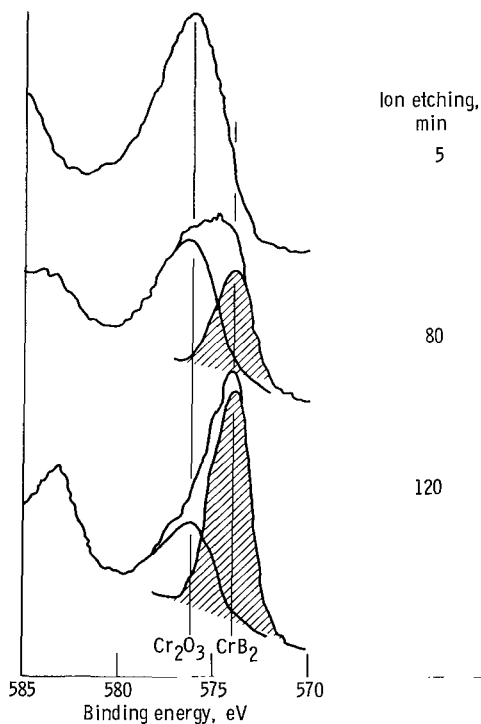


Figure 7. - Cr(2p 3/2) XPS peak in  $\text{CrB}_2$  film sputtered at 600 watts, -500 volts bias for 10 minutes sputter etched for 5, 80, and 120 minutes. (See table I for  $\text{Cr}_2\text{O}_3$  and  $\text{CrB}_2$  reference values. Curve resolver used to determine component peaks shown.)

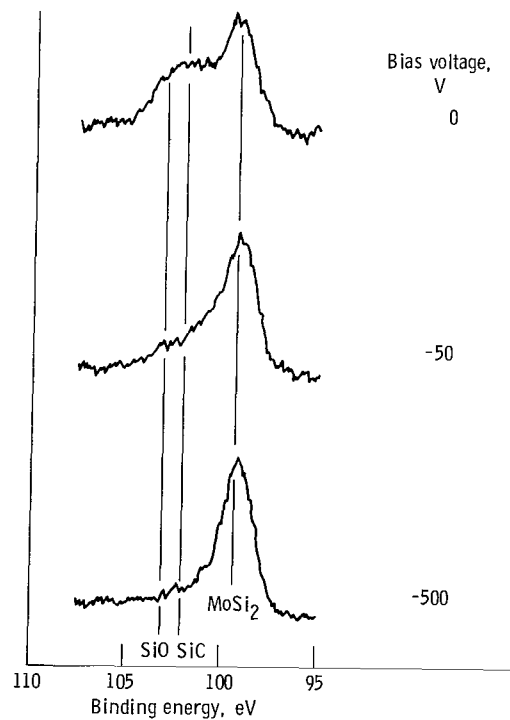


Figure 8. - Silicon (2p) XPS peak in  $\text{MoSi}_2$  film sputtered at three different bias voltages. Measured after 10 minutes argon ion sputter etching films deposited at 300 watts for 20 minutes. (See table I for  $\text{SiO}_2$  and SiC reference values.)

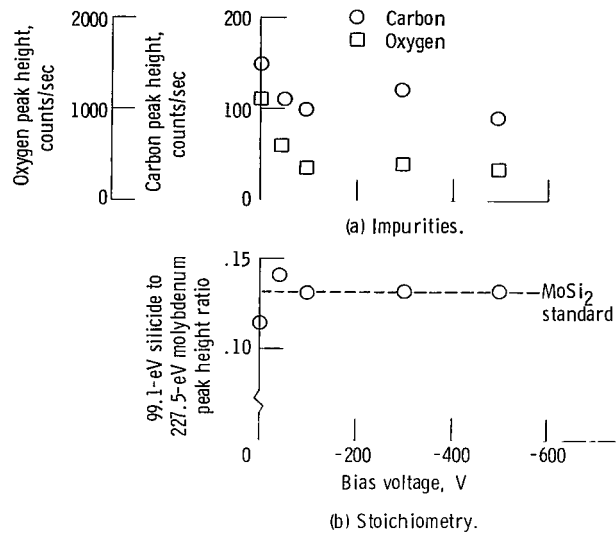


Figure 9. - Influence of bias voltage on MoSi<sub>2</sub> coatings.

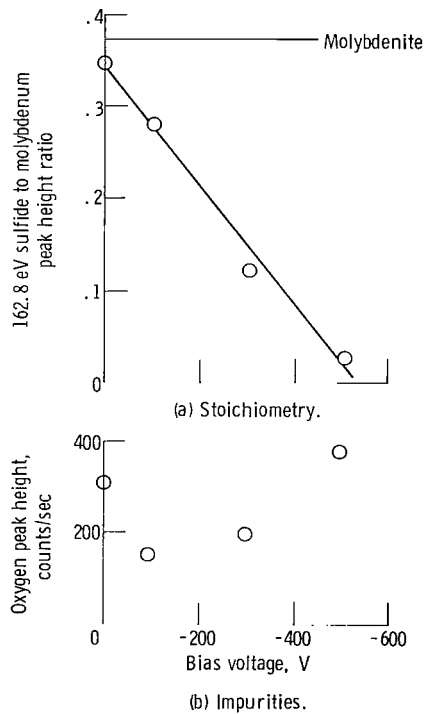


Figure 10. - Influence of bias voltage on MoS<sub>2</sub> coatings.

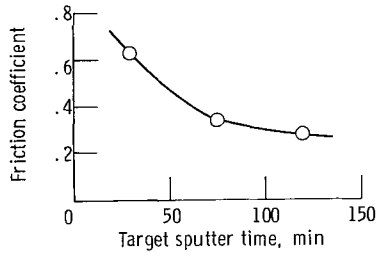


Figure 11. - Friction coefficient for rf sputtered  $\text{CrB}_2$  coatings on 440-C disks, 304 riders as a function of target history; 25 gram load;  $\text{N}_2$  atmosphere; 0 volt bias; 10 minutes deposition.

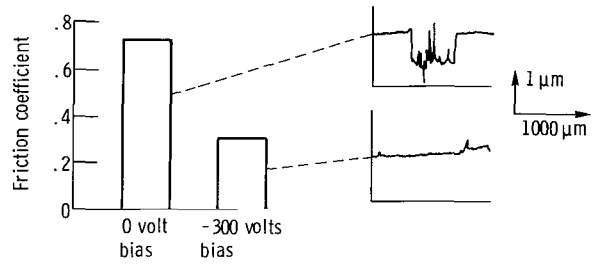


Figure 12. - Friction coefficient and wear tracings for  $\text{CrB}_2$  coated 440-C disks with 304 rider; 25 gram load;  $\text{N}_2$  atmosphere; 40 minutes deposition.

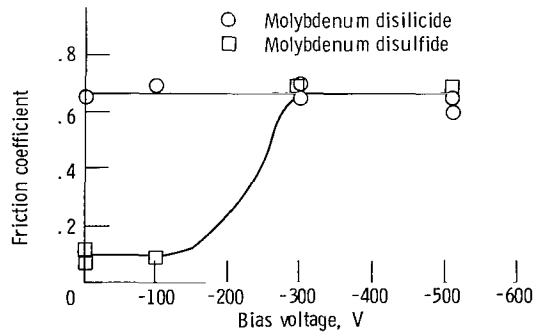


Figure 13. - Friction coefficients for rf sputtered films on 440-C disks; 304 rider;  $\text{N}_2$  atmosphere; load, 10 grams.



542 001 C1 U C 770/28 S00903DS  
DEPT OF THE AIR FORCE  
AF WEAPONS LABORATORY  
ATTN: TECHNICAL LIBRARY (SUL)  
KIRTLAND AFB NM 87117

POSTMASTER: If Undeliverable (Section 158  
Postal Manual) Do Not Return

*"The aeronautical and space activities of the United States shall be conducted so as to contribute . . . to the expansion of human knowledge of phenomena in the atmosphere and space. The Administration shall provide for the widest practicable and appropriate dissemination of information concerning its activities and the results thereof."*

—NATIONAL AERONAUTICS AND SPACE ACT OF 1958

## NASA SCIENTIFIC AND TECHNICAL PUBLICATIONS

**TECHNICAL REPORTS:** Scientific and technical information considered important, complete, and a lasting contribution to existing knowledge.

**TECHNICAL NOTES:** Information less broad in scope but nevertheless of importance as a contribution to existing knowledge.

**TECHNICAL MEMORANDUMS:** Information receiving limited distribution because of preliminary data, security classification, or other reasons. Also includes conference proceedings with either limited or unlimited distribution.

**CONTRACTOR REPORTS:** Scientific and technical information generated under a NASA contract or grant and considered an important contribution to existing knowledge.

**TECHNICAL TRANSLATIONS:** Information published in a foreign language considered to merit NASA distribution in English.

**SPECIAL PUBLICATIONS:** Information derived from or of value to NASA activities. Publications include final reports of major projects, monographs, data compilations, handbooks, sourcebooks, and special bibliographies.

**TECHNOLOGY UTILIZATION PUBLICATIONS:** Information on technology used by NASA that may be of particular interest in commercial and other non-aerospace applications. Publications include Tech Briefs, Technology Utilization Reports and Technology Surveys.

*Details on the availability of these publications may be obtained from:*

**SCIENTIFIC AND TECHNICAL INFORMATION OFFICE**

**NATIONAL AERONAUTICS AND SPACE ADMINISTRATION**

**Washington, D.C. 20546**